Climate data selection for multi-decadal wind power forecasts

Sofia Morelli, Nina Effenberger, Luca Schmidt, Nicole Ludwig

Angaben zur Veröffentlichung / Publication details:

Morelli, Sofia, Nina Effenberger, Luca Schmidt, and Nicole Ludwig. 2025. "Climate data selection for multi-decadal wind power forecasts." *Environmental Research Letters* 20 (4): 044032. https://doi.org/10.1088/1748-9326/adc01f.

ENVIRONMENTAL RESEARCH
LETTERS

LETTER • OPEN ACCESS

Climate data selection for multi-decadal wind power forecasts

To cite this article: Sofia Morelli *et al* 2025 *Environ. Res. Lett.* **20** 044032

IOP Publishing Environ. Res. Lett. 20 (2025) 044032 https://doi.org/10.1088/1748-9326/adc01f

ENVIRONMENTAL RESEARCH
LETTERS

RECEIVED
19 November 2024

REVISED
24 February 2025

ACCEPTED FOR PUBLICATION
13 March 2025

PUBLISHED
25 March 2025

LETTER

Climate data selection for multi-decadal wind power forecasts

Sofia Morelli[1,2,3], Nina Effenberger[1,3], Luca Schmidt[1,3,*] and Nicole Ludwig[1]

[1] Cluster of Excellence Machine Learning, University of Tübingen, Tübingen, Germany
[2] Methods Center, University of Tübingen, Tübingen, Germany
[3] Equal contribution.
[*] Author to whom any correspondence should be addressed.

E-mail: luca.schmidt@uni-tuebingen.de, sofia.morelli@uni-tuebingen.de, nina.effenberger@env.ethz.ch and nicole.ludwig@uni-tuebingen.de

Keywords: spatial resolution, climate model, wind speed, wind power

Abstract

Reliable wind speed data is crucial for applications such as estimating local (future) wind power. Global climate models (GCMs) and regional climate models (RCMs) provide forecasts over multi-decadal periods. However, their outputs vary substantially, and higher-resolution models come with increased computational demands. In this study, we analyze how the spatial resolution of different GCMs and RCMs affects the reliability of simulated wind speeds and wind power, using ERA5 data as a reference. We present a systematic procedure for model evaluation for wind resource assessment as a downstream task. Our results show that while a high spatial resolution can improve the representation of wind speed characteristics, notably extremes, the model choice is more critical for capturing the full wind speed distribution and corresponding power generation. The *IPSL* model preserves the wind speed distribution particularly well in Europe, producing the most accurate wind power forecasts relative to ERA5 data. Therefore, selecting the right GCMs and RCMs should precede considerations of spatial resolution or GCM boundary conditions. However, higher resolution can be valuable once a suitable climate model is identified.

1. Introduction

Wind is expected to become a dominant source of energy in future power supply (IEA). For wind to be a reliable energy source, accurate regional wind forecasts over multi-decadal periods are necessary. Climate model output is a natural choice of data for such analyses, as they provide projections on multi-decadal timescales (e.g. Pryor *et al* 2020, Ndiaye *et al* 2022). Climate models are complex physical earth system models whose outputs can differ substantially with large inherent model uncertainties (Zhang and Wang 2024). Given this variability, it is crucial to assess the skill of climate models, especially their ability to perform in specific applications of interest such as wind power forecasting (Moemken *et al* 2016, Isphording *et al* 2024).

Previous research revealed that a higher spatial resolution of wind data is desirable. Not only because it provides more local forecasts (Rummukainen 2016), but because the resolution at which a model operates affects which weather phenomena it can resolve (Lucas-Picher *et al* 2021). While higher-resolution models can resolve more fine-grained weather phenomena, they come with computational challenges. All models–no matter the spatial resolution–require modeling assumptions and, therefore, contain errors and uncertainties. It remains unclear which climate data, at which spatial resolution, best represents future wind speeds.

There are techniques to increase the spatial resolution of global climate model (GCM) output. Regional climate models (RCMs) use GCMs as their input and run at finer resolution (Vautard *et al* 2021) to physically resolve more fine-grained weather phenomena. This process, called dynamical downscaling, is, however, computationally intensive. Statistical downscaling methods offer a less resource-demanding alternative, establishing relationships between low-resolution GCM output and localized weather patterns (e.g. Schmidt and Ludwig 2024). However, these methods still require high-resolution data to establish such a relationship. While RCMs and statistical downscaling techniques can add value in regions with complex terrain or significant land-sea contrasts, they do not always outperform raw GCM data (Rummukainen 2016). Furthermore, for CMIP6, no unified collection of RCM data is available. Given these data limitations, it is necessary to investigate whether raw GCM data from CMIP6 can still be valuable for multi-decadal wind power forecasts-despite their lower spatial resolution.

The value of climate models is difficult to assess as climate model outputs are not spatio-temporally aligned. Comparing climate model output to reanalyzes such as ERA5 is, therefore, non-trivial. Typically, climate models are validated based on aggregate statistics using their historical runs (e.g. Randall *et al* 2007). In the context of wind power evaluation, an additional challenge arises as the actual variable of interest–wind power–is derived. The variable climate models project is wind speed, and the relationship between power and speed is complex. To still account for the known non-linearities, other research considers wind speeds cubed (Miao *et al* 2023), simulates load factors (MacLeod *et al* 2018) or transforms wind speeds to wind power using a turbine power curve (Ko *et al* 2022).

In the following, we investigate historical wind speeds and derived wind power to analyze how the spatial resolution of global and RCM data affects multi-decadal wind power forecasts. In section 2 we explain how we evaluate different wind (power) projections, in section 3 we describe our results and in section 4 we discuss our results, shortcomings and future work.

2. Methods

To compare the influence of climate model resolution on multi-decadal wind power forecasts, we investigate wind speeds using climate models and subsequent wind power predictions. In the following, we describe the data we use and our evaluation approach.

2.1. Data

In our analysis, we compare the reanalysis dataset ERA5 (Hersbach *et al* 2020) to GCM data from ten CMIP6 models (Eyring *et al* 2016) as well as RCM data from CORDEX (Giorgi and Gutowski Jr 2015) based on CMIP5 global boundary models (Taylor *et al* 2012). An overview of all GCMs and RCMs used can be found in tables A.1 and A.2, respectively. We use wind velocities u and v at six-hourly instantaneous resolution as these were found to be reliable for multi-decadal predictions in Effenberger *et al* (2023) and compute wind speeds w as

$$w = \sqrt{u^2 + v^2}. \tag{1}$$

Our study region covers all data points in continental Europe within a rectangle with longitudes $\in [25°, 73°]$ and latitudes $\in [-30°, 42°]$. This means we consider gridded data over land of different resolutions, as shown in figure 1. We focus on historical runs of climate models from 2005 to 2015. We choose the first ensemble member run typically labeled as `r1i1p1f1` on the CMIP6 ESGF server. To maintain consistency and due to the lack of data from higher elevations in CMIP6, we use wind speeds w_{10} at 10 m above ground from both ERA5 and CMIP6. For MPI CMIP5, the only available six-hourly wind speed data at the time of study, provided on the ESGF node (Giorgetta *et al* 2012), were at an altitude of 1500 m. Therefore, we replace w_{10} by w_{1500} in the power law to extrapolate the CMIP5 GCM model data to 126 m, the hub height of the assumed wind turbine. To ensure consistency, we extrapolate all wind speed data to this height before estimating wind power. In figure A.2 we show results for other turbines and hub heights. To extrapolate the wind speeds to 126 m we use a wind profile power law following

$$w_{126} = \left(\frac{126}{10}\right)^{\alpha} \cdot w_{10}, \tag{2}$$

where the coefficient α is empirically derived to be about $\frac{1}{7}$ for neutral stability conditions (Peterson and Hennessey 1978). For ERA5, we use the original data on a reduced Gaussian grid. Since the regional model runs from CMIP5 are on a curvilinear grid, we regrid them to a regular Gaussian grid with a matching spatial resolution (0.1°) using bilinear interpolation (Schulzweida 2023).

Although ERA5 is widely recognized as a reasonable reference (Ramon *et al* 2019, Kaspar *et al* 2020) and is shown to be superior to other reanalysis datasets (Olauson 2018, Molina *et al* 2021), it still contains notable biases, particularly underestimating wind speeds (Gualtieri 2021), which can affect wind power simulations (Staffell and Pfenninger 2016). Ideally, observational wind speed data at turbine hub height would be used to validate climate model simulations. However, such datasets are typically not available for larger regions (Effenberger and Ludwig 2022) and our analysis relies on gridded data. Given these constraints, we rely on ERA5 as a widely used reanalysis product, despite known biases (Gualtieri 2021).

2.2. Evaluation and metrics

The evaluation is performed on two aspects: wind speed and wind power. While wind power is our ultimate variable of interest, the analysis centers primarily around wind speed, the variable provided by the climate models. Wind power can be estimated from wind speed using a theoretical wind power curve. Due to the non-linear nature of this relationship, however, a comprehensive analysis of wind speed distributions is essential for understanding its implications for wind power.

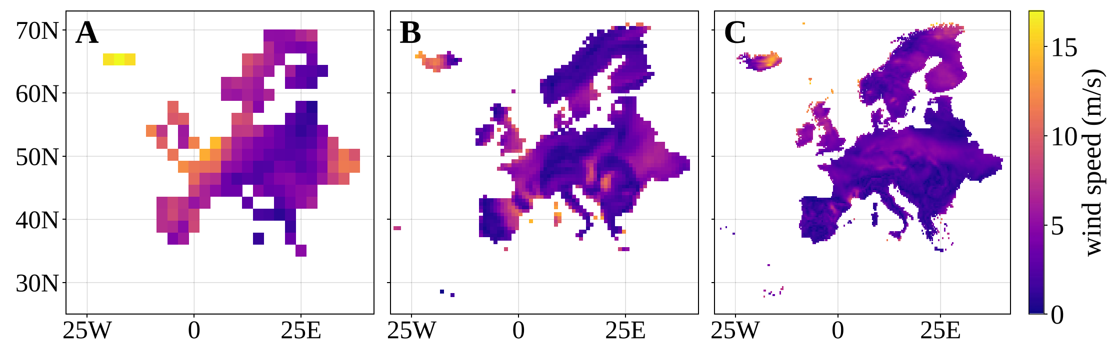

Figure 1. Example of gridded wind speed data over Europe with varying grid sizes. A single time frame of the same day (01.01.2005) of the lowest resolution CMIP6 dataset NCC-LR (A), the highest resolution CMIP6 dataset MOHC-HR (B), and the ERA5 reanalysis dataset (C) is shown to illustrate the differences in spatial resolution across datasets.

2.2.1. Wind speed distributions

We investigate kernel density estimations (KDEs) and use quantitative methods to compare and analyze wind speed distributions. Since there is no universal metric for comparing distributions, we employ the Jensen–Shannon distance and the Wasserstein-1 distance, each providing a distinct approach to quantifying differences between distributions.

KDEs

We estimate the wind speed probability distributions using KDE

$$\mathrm{KDE}(w) = \frac{1}{nh}\sum_{i=1}^{n} K\left(\frac{w - w_i}{h}\right), \tag{3}$$

using Scott's rule (Scott 2010) to select a bandwidth h and the Gaussian kernel $K(x)$

$$K(x) = \frac{1}{\sqrt{2\pi}}\exp\left(-\frac{1}{2}x^2\right). \tag{4}$$

Jensen–Shannon (JS) distance

We use the JS distance to measure how closely a GCM's KDE wind speed distribution aligns with the ERA5 KDE wind speed distribution. This metric is a symmetric and smooth variant of the Kullback–Leibler (KL) divergence (Endres and Schindelin 2003), and is defined as

$$\mathrm{JS}(P_{\mathrm{ref}}, P_{\mathrm{pred}}) = \sqrt{\frac{1}{2}\mathrm{KL}(P_{\mathrm{ref}} \parallel M) + \frac{1}{2}\mathrm{KL}(P_{\mathrm{pred}} \parallel M)}, \tag{5}$$

where M is the mixture distribution

$$\mathrm{M} = \frac{1}{2}(P_{\mathrm{ref}} + P_{\mathrm{pred}}), \tag{6}$$

and $\mathrm{KL}(P_{\mathrm{ref}} \parallel P_{\mathrm{pred}})$ is the KL divergence between the reference distribution P_{ref} and the predicted distribution P_{pred}, defined as

$$\mathrm{KL}(P_{\mathrm{ref}} \parallel P_{\mathrm{pred}}) = \sum_{x \in \mathcal{X}} P_{\mathrm{ref}}(x)\log\left(\frac{P_{\mathrm{ref}}(x)}{P_{\mathrm{pred}}(x)}\right). \tag{7}$$

An advantage of the JS distance is that there are no issues related to undefined or infinite values when comparing distributions with zero wind speeds. Additionally, the JS distance is bounded between $[0,1]$ (unlike the Wasserstein-1 distance), offering an intuitive interpretation of the results as a similarity measure.

Wasserstein-1 distance

As an additional way to compare the wind speed distributions between the GCMs and ERA5 we use the Wasserstein-1 (W1) distance. The metric is based on the concept of *optimal transport* and differs from JS distance in interpretation and mathematical properties. The W1 distance is defined as

$$\mathrm{W}(P_{\mathrm{pred}}, P_{\mathrm{ref}}) = \inf_{\gamma \in \Pi(P_{\mathrm{pred}}, P_{\mathrm{ref}})} \mathbb{E}_{(x,y)\sim\gamma}\left[\|x - y\|_1\right], \tag{8}$$

where $\Pi(P_{\mathrm{pred}}, P_{\mathrm{ref}})$ is the set of couplings, i.e. joint distributions whose marginals are P_{pred} and P_{ref}. Conceptually, the W1 distance quantifies the expected cost of the optimal transport plan that transforms the distribution P_{pred} into P_{ref} (Arjovsky *et al* 2017).

Range analysis

Additionally, we analyze the range of wind speeds the models can resolve to understand their overall ability to project wind speeds independently of the power curve. Since the lower bound of wind speeds is 0 m s^{-1}, our focus is on the upper tail of the distribution. We expect very high wind speeds to be linked with spatial resolution, as higher-resolution models may better capture more complex atmospheric processes, potentially leading to a more accurate representation of extreme events (Outten and Sobolowski 2021). To evaluate the models' ability to project high wind speeds, we calculate the average of the 100 highest wind speeds for each model respectively. Percentile-based evaluation is avoided, as differences in model resolution would result in varying data points for the same percentile across models.

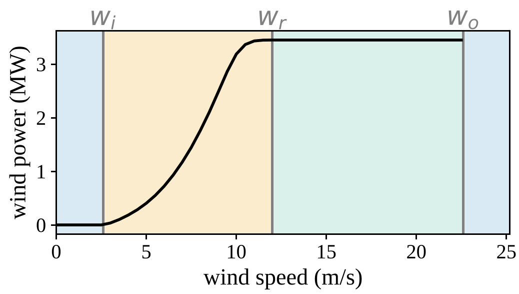

Figure 2. Power curve of the `Vestas V126-3.45` turbine. No power is generated for wind speeds below the cut-in wind speed w_i and above the cut-off wind speed w_o. For $w \in [w_i, w_r]$, the relationship between wind speed and power is almost cubic. Between w_r and w_o the power output remains constant at its maximum.

Linear regression
The CMIP6 datasets differ in their latitude and longitude coordinates, and we use the number of spatial points within the selected area to measure the grid resolution. To examine trends in distance metrics and maximum wind speeds with increasing spatial resolutions, we perform linear-log regression (Montgomery *et al* 2021). We can then describe the distance of each model to ERA5 as a function of the resolution r

$$w_{max}(r) = \beta_0 + \beta_1 \log(r) + \epsilon, \tag{9}$$

where $\epsilon \sim \mathcal{N}(0, \sigma^2)$ is Gaussian noise and β_0 and β_1 are computed using the method of least squares.

2.2.2. Wind power estimation
So far, we focused on wind speed, as wind directions are a direct output from GCMs. However, wind power is our variable of interest, and its estimation involves assumptions and simplifications. While wind speed is a proxy, the ultimate goal is to understand how variations in wind speed distributions impact (multi-decadal) wind power estimation. To compute the wind power generation at each grid point, we input the wind speeds at grid points into a wind turbine power curve (Haas *et al* 2024). In the main part of the paper, we choose the `Vestas V126-3.45` wind turbine power curve with a hub-height of 126m, see figure 2. Supporting results for other turbines are provided in appendix. We compute the cumulative wind power generation by summing the power generation of all time steps and grid points over land in each dataset. To enable a comparison of relative cumulative wind power estimates across different models, the power predictions from the climate models are normalized by those from ERA5.

3. Results

We investigate the spatial resolution of GCMs and compare the wind power predicted by different RCMs. Our results reveal that the choice of the underlying physical model- whether an RCM or GCM- is influential, and we do not find systematic trends with increasing resolution except in the representation of very high wind speeds.

3.1. Higher resolution of GCM does not imply better forecast

The results in figure 3 reveal substantial differences in the estimated wind speed KDEs and corresponding wind power across models. For instance, the NCC model shows a much greater wind speed distribution spread than ERA5.

3.1.1. Wind speed analysis
We analyze the JS and W1 distance of the GCMs and ERA5 to quantify these distributional differences in wind speeds, as shown in figure 4. These metrics show substantial variability in the ability of each model to capture the wind speed distribution accurately. However, regression analysis shows no statistically significant linear relationship between the two metrics considered and spatial resolution. This suggests that while the accuracy of wind speed distributions varies substantially between models, this variation is not systematically linked to spatial resolution.

Range analysis
Initially, we identify extreme wind speeds using the cut-in and cut-out values of the power curve as thresholds. This analysis reveals large variability between models, but again, this variability is not systematically linked to spatial resolution; see the results in appendix. While these values are important for wind power generation, they do not represent meteorological extremes. To better understand the range of wind speeds the models can generate, we focus on extremes defined by the average of the 100 highest wind speeds per model. While all models except the NCC model generate zero wind speeds, the upper tail shows much greater variation between models. The regression between these highest wind speeds and the logarithm of spatial resolution is significant at the 5% level, indicating a positive relationship between spatial resolution and a model's ability to represent high wind speeds. This trend is especially evident in models with both high- and low-resolution versions, where high-resolution models (MPI, MOHC, NCC) consistently generate higher wind speeds, see figure 5.

3.1.2. Wind power analysis
When wind speeds are converted to wind power, accurately capturing specific wind speed quantiles becomes critical. Despite this, the cumulative wind power estimated for ten years, shown as a percentage relative to ERA5 power output in figure 6, reflects similar trends as observed in the wind speed distributions. There is considerable variation in the estimated cumulative wind power across different models, with

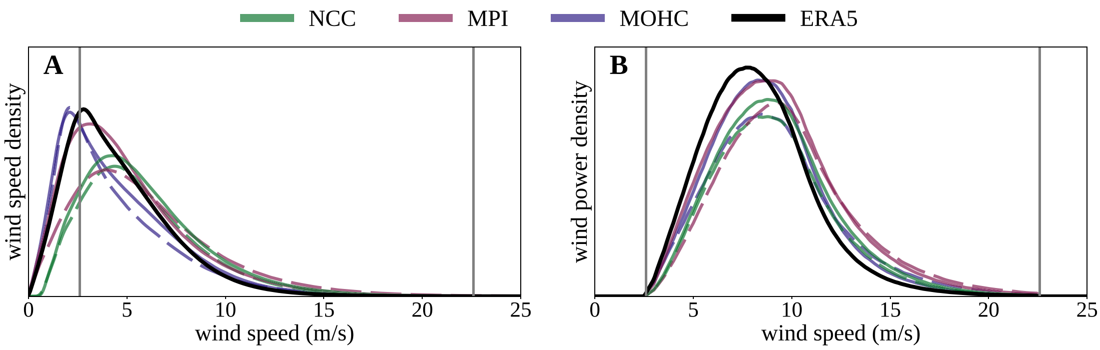

Figure 3. Kernel density estimations (KDEs) of the wind speeds (A) and the corresponding generated wind power density (B) calculated using the wind speed KDEs as input to the wind turbine power curve. ERA5 (black line) and GCM datasets available at different resolutions are displayed, where dashed lines indicate the low-resolution version (KDEs of all GCM datasets are shown in figure A.1). Vertical grey lines indicate the cut-in and cut-off wind speeds of the `Vestas V126-3.45` turbine at 2.6 m s^{-1} and 22.6 m s^{-1}, respectively. While most wind speeds are $<$10 m s^{-1}, most of the wind power is generated by wind speeds $\sim$10 m s^{-1}.

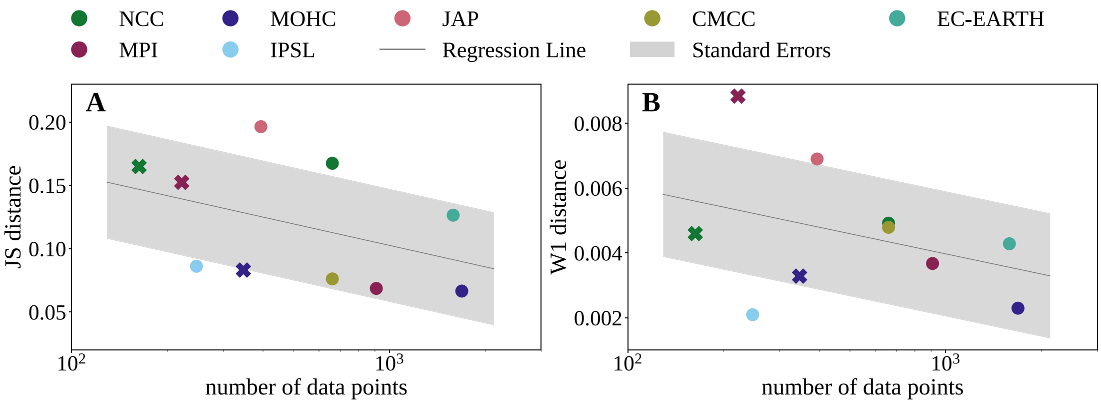

Figure 4. The JS distance (A) and the W1 distance (B) between the wind speed samples from CMIP6 and ERA5 are plotted against the spatial resolution (values are provided in table A.3). When datasets of the same model with different resolutions are available, the low-resolution version is indicated by a cross instead of a circle. The gray line represents the linear-log regression fit with standard errors. The regressions in (A) and (B) are both not statistically significant at the 5% significance level (see table A.4).

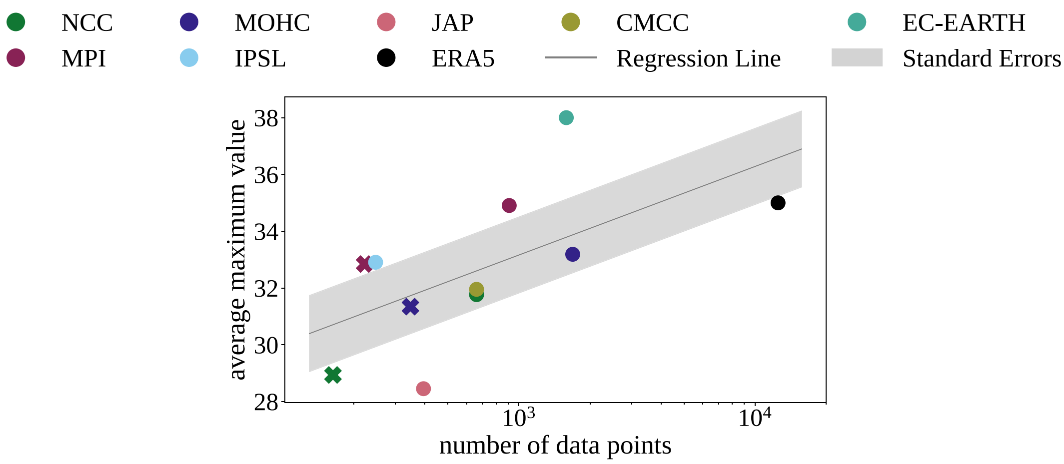

Figure 5. The average over the 100 highest wind speed values per model is plotted against the spatial resolution (values are provided in table A.3). The linear-log regression shows a statistically significant positive relationship (at the 5% level) between spatial resolution and the model's ability to represent extremely high wind speeds (see table A.4). For all models that offer low- and high-resolution versions, the higher-resolution dataset represents greater extremes (compare crosses and dots of the same color).

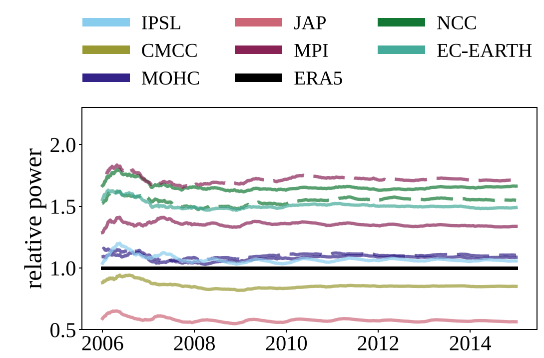

Figure 6. Cumulative power of CMIP6 datasets relative to ERA5. When datasets with different resolutions run by the same model exist, the low-resolution version is indicated with a dashed line. The choice of GCM substantially influences the power prediction; most GCMs overestimate wind power relative to ERA5.

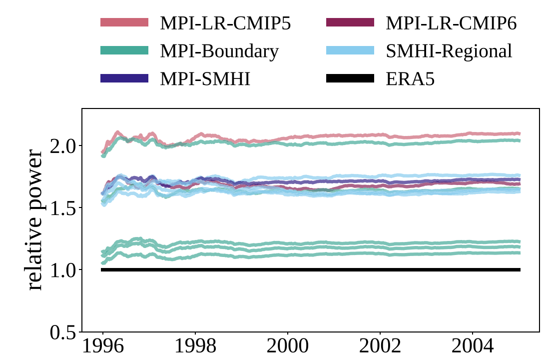

Figure 7. Cumulative power of CMIP5 regional and CMIP6 MPI from 1995 to 2005 relative to ERA5. The spread of the cumulative wind power predictions from multiple RCMs using the output of the MPI model as boundary conditions is larger than the spread using one RCM with different boundary conditions.

eight models overestimating wind power output relative to ERA5, while two models underestimate it.

Furthermore, the relative cumulative power forecasts differ greatly, ranging from -42.56% to 68.16% compared to ERA5. For example, the GCM IPSL aligns most closely with ERA5. Meanwhile the forecasts from the raw GCM data of CMCC and MOHC fall within a range that could be useful for practical applications.

3.2. RCM choice significantly influences the forecast

We further investigate regional model data from CMIP5 and present the corresponding results in figure 7. For the global model run of the MPI CMIP5 model, we extrapolate data to a different height (see section 2). CMIP5 predictions overestimate wind power the most compared to ERA5. In contrast, all regional model runs and the CMIP6 model run are closer to ERA5. Comparing the spread of the predictions from the MPI model that is downscaled with several regional models (cyan in figure 7) to the prediction of several GCMs downscaled with the regional model SMHI (light blue in figure 7) reveals that the spread of different RCMs is greater than that of one regional model with different boundary conditions. This is also reflected in the variance of the relative power predictions, which is 10.87% for the regional models with the same boundary conditions and 0.26% for the MPI model with different boundary conditions.

4. Discussion

In this study, we evaluate how GCM's spatial data resolution affects the reliability of simulated wind speeds for multi-decadal wind power forecasts. Specifically, we focus on ten raw ensemble members of different CMIP6 GCMs over the period 2005 – 2015, comparing wind speed simulations and derived wind power estimates for the European region with ERA5 reanalysis data. Contrary to the common assumption that higher resolution provides more reliable wind speeds (Pryor *et al* 2012, Molina *et al* 2022), we do not find a clear trend in wind accuracy with increasing spatial resolution. Instead, we observe that the accuracy of wind speed simulations varies substantially between different models. Additionally, we investigate the performance of several regional models from CMIP5, finding only a small spread in predictions when using different boundary conditions with the same RCM. However, a much larger spread is visible when comparing different RCMs, again emphasizing the importance of model choice. Analysis of wind speed distributions shows that high-resolution models are better at capturing the upper tails of the distribution. Furthermore, higher-resolution versions of the same climate model better capture extremes relative to their lower-resolution counterparts. Therefore, a higher spatial resolution is desirable—once a suitable climate model has been selected.

In line with this rationale, we refrain from applying bias correction or downscaling in our analysis, recognizing that these techniques cannot correct fundamental model misrepresentations and may even disrupt the internal consistency of the climate models (Maraun 2016, François *et al* 2020). Our findings are consistent with other studies emphasizing the importance of high-quality, high-resolution models for accurate wind speed simulations (Pryor *et al* 2023), particularly for resolving fine-scale phenomena, such as extreme wind events. A high resolution is necessary to accurately resolve topographic features like surface roughness and elevation (Beniston *et al* 2007, Yu *et al* 2022). Increasing the resolution through dynamical downscaling has also proven beneficial for predicting future capacity factors at individual turbine sites (Pryor *et al* 2023). However, increasing spatial resolution alone does not guarantee an improved representation of these complex processes. This aligns with findings on effective resolution (Klaver *et al* 2020), where increases in spatial resolution do not proportionally translate into enhanced representation of meteorological phenomena. Additionally, the accuracy of wind speed simulations is influenced by several interacting factors, such as how changes in land use, external forcings, and internal variability are modeled (Wohland *et al* 2019) and how physical parameterizations, such as the planetary boundary layer scheme, land surface representation, and surface roughness length, are implemented (Hahmann *et al* 2020).

Our analysis indicates that the IPSL model performs exceptionally well in simulating wind speeds and wind power over Europe, while the MPI-LR model performs the least well. However, our findings are likely region-specific and several limitations must be considered. For example, we simplify our analysis by modeling wind power with a theoretical power curve and interpolating near-surface wind speeds vertically using a power law with $\alpha = \frac{1}{7}$ to model wind speeds at a standard hub height. Using such a power law for vertical interpolation has been criticized (Barthelmie *et al* 2020). For example, Pryor *et al* (2023) recommend using wind speeds at hub height rather than relying on 10 m wind speeds, still, they acknowledge that observational datasets at these heights remain scarce. Due to the lack of high met mast wind data (Effenberger and Ludwig 2022) as well as CMIP6 data at hub heights, we adopt the approach of consistently using the power law with 10 m data as commonly done in the literature (Shu and Jesson 2021). Future work should focus on integrating additional data sources, such as downscaled climate data and actual power generation data.

Given the results, we advocate for prioritizing model choice over spatial resolution when choosing models for multi-decadal wind power forecasts. While CMIP6 may have a coarser resolution, it offers notable advancements over its predecessor, CMIP5, in simulating climate dynamics and providing more reliable multi-decadal forecasts (Miao *et al* 2023). Therefore, selecting an appropriate climate model should be approached case-by-case, guided by a systematic procedure like the one we present in this paper.

5. Conclusion

Climate information is essential for multi-decadal wind power forecasting. Available climate models, among other things, vary substantially in their spatial resolution. We analyze 10 global and additional RCMs for their ability to predict long-term wind power.

Our findings highlight the need for high-quality GCMs and RCMs, particularly for wind energy planning. Given the sensitivity of wind power generation to local climate conditions, it is essential that models accurately capture both large-scale dynamics and more local meteorological phenomena. Higher-resolution climate models enhance the representation of extreme wind speeds, yet they do not guarantee improved accuracy in wind speed forecasts. Instead, the selection of the climate models, both GCM and RCM, emerges as a more influential factor for wind speed and power predictions than the spatial resolution itself. As we do not find substantial differences between CMIP5 regional models and CMIP6 global models, we recommend selecting climate models from CMIP6 for multi-decadal wind speed forecasts, as they offer the most current advancements in climate modeling.

Data availability statement

All data is open-source, and the code is available at https://github.com/sofiamorelli/erl_2025.

Acknowledgments

This research was funded by the Deutsche Forschungsgemeinschaft (DFG, German Research Foundation) under Germany's Excellence Strategy—EXC Number 2064/1—Project Number 390727645, and the Tübingen AI Center. The authors thank the International Max Planck Research School for Intelligent Systems (IMPRS-IS) for supporting Nina Effenberger and Luca Schmidt.

Appendix. Supplementary information

A.1. Climate model details

We provide an overview and additional details on the GCMs from CMIP6 and RCMs from CORDEX used in this study. Table A.1 summarizes the atmospheric components, spatial resolution, and land-based data coverage of the CMIP6 models, while table A.2 presents the CORDEX datasets, listing the global boundary models alongside their corresponding regional models. Additionally, table A.3 summarizes key wind speed characteristics relevant to wind power generation.

Table A.1. CMIP6 datasets: Labels as used in this paper (first column), names of atmospheric model components (second column), original spatial resolutions in terms of grid specification (third column), number of data points when selecting the land mass of Europe (fourth column), and native resolution (fifth column) as indicated in the references given in the last column.

Label	Model	Grid Resolution	Number of Data Points	Native Resol.	Reference
CMCC	CM2-SR5	$0.9° \times 1.25°$	661	100 km	Lovato and Peano (2020)
EC-EARTH	EC-Earth3.3	T255	1586	100 km	EC-Earth (2019)
IPSL	CM6A-LR	$2.5° \times 1.3°$	247	250 km	Boucher *et al* (2018)
JAP	MIROC6	T85	394	250 km	Tatebe and Watanabe (2018)
MOHC-LR	HadGEM3-GC31-LL	N96	347	250 km	Ridley *et al* (2019b)
MOHC-HR	HadGEM3-GC31-MM	N216	1688	100 km	Ridley *et al* (2019a)
MPI-LR	ESM1.2-LR	T63	222	250 km	Wieners *et al* (2019)
MPI-HR	ESM1.2-HR	T127	909	100 km	Jungclaus *et al* (2019)
NCC-LR	NorESM2-LM	$2.5° \times 1.875°$	163	250 km	Seland *et al* (2019)
NCC-HR	NorESM2-MM	$1.25° \times 0.9375°$	661	100 km	Bentsen *et al* (2019)
MPI-LR-CMIP5	ECHAM6	T63	222	200 km	Giorgetta *et al* (2012)
ERA5	IFS CY41R2	$0.25° \times 0.25°$	12 506		Hersbach *et al* (2020)

Table A.2. CORDEX datasets: Labels of the global boundary models (first column) and their full model names (second column), labels of the regional models (third column) and their full model names (fourth column). All datasets have resolution $0.11° \times 0.11°$ 12.5 km and were withdrawn from Copernicus Climate Change Service (2019).

Label GCM	Model	Label RCM	Model
MPI	MPI-M-MPI-ESM-LR	CNRM	CNRM-ALADIN63
MPI	MPI-M-MPI-ESM-LR	DMI	DMI-HIRHAM5
MPI	MPI-M-MPI-ESM-LR	ETH	CLMcom-ETH-COSMO-crCLIM
MPI	MPI-M-MPI-ESM-LR	ICTP	ICTP-RegCM4-6
MPI	MPI-M-MPI-ESM-LR	MOHC	MOHC-HadREM3-GA7-05
MPI	MPI-M-MPI-ESM-LR	SMHI	SMHI-RCA4
MOHC	MOHC-HadGEM2-ES	SMHI	SMHI-RCA4
NCC	NCC-NorESM1-M	SMHI	SMHI-RCA4
IPSL	IPSL-CM5A-MR	SMHI	SMHI-RCA4
EC-EARTH	ICHEC-EC-EARTH	SMHI	SMHI-RCA4
CNRM	CNRM-CERFACS-CM5	SMHI	SMHI-RCA4

Table A.3. Characteristics of the datasets listed in table A.1: the mean wind speed (second column), the Jensen-Shannon (JS) distance to ERA5 (third column), the Wasserstein-1 (W1) distance to ERA5 (fourth column), the average over the 100 highest wind speed values (fifth column), the percentage of zero power values due to wind speed values below the cut-in at 2.6 m s^{-1} (sixth column), and the percentage of zero power values due to wind speed values above the cut-off at 22.6 m s^{-1} (seventh column).

Model	Mean	JS distance	W1 distance	Max average	Low value %	High value %
CMCC	4.32	0.076	0.005	31.95	27.50	0.030
EC-EARTH	5.54	0.126	0.004	38.00	14.40	0.111
IPSL	4.56	0.086	0.002	32.91	31.34	0.079
JAP	3.37	0.196	0.007	28.45	47.33	0.010
MOHC-LR	4.50	0.083	0.003	31.34	32.69	0.056
MOHC-HR	4.55	0.067	0.002	33.19	30.89	0.025
MPI-LR	5.92	0.152	0.009	32.84	16.62	0.150
MPI-HR	5.05	0.069	0.004	34.91	23.17	0.061
NCC-LR	5.80	0.165	0.005	28.94	12.07	0.041
NCC-HR	5.84	0.167	0.005	31.77	12.11	0.040
ERA5	4.58	—	—	35.00	24.80	0.015

A.2. Wind speed analysis details

We present additional results related to the wind speed analysis. Table A.4 provides the regression parameters corresponding to figure 4 in the main paper. Furthermore, figure A.1 shows the wind speed and wind power KDEs for all models, including those omitted in the main part of the paper for clarity.

Table A.4. Regression details for the Jensen-Shannon (JS) and the Wasserstein-1 (W1) distance, and the average over the 100 highest wind speed values; including the regression parameters α (second column) and β (third column), the standard error of the slope (fourth column), the explained variance ($100 \cdot R^2$) in % (fifth column) and the p-value of the Overall-F-Test (sixth column).

	Intercept α	Slope β	Std. Dev.	R^2	p-value
JS distance	0.271	−0.056	0.044	16.698	0.241
W1 distance	0.010	−0.002	0.002	12.647	0.313
Max Average	23.807	3.119	1.339	37.626	0.045

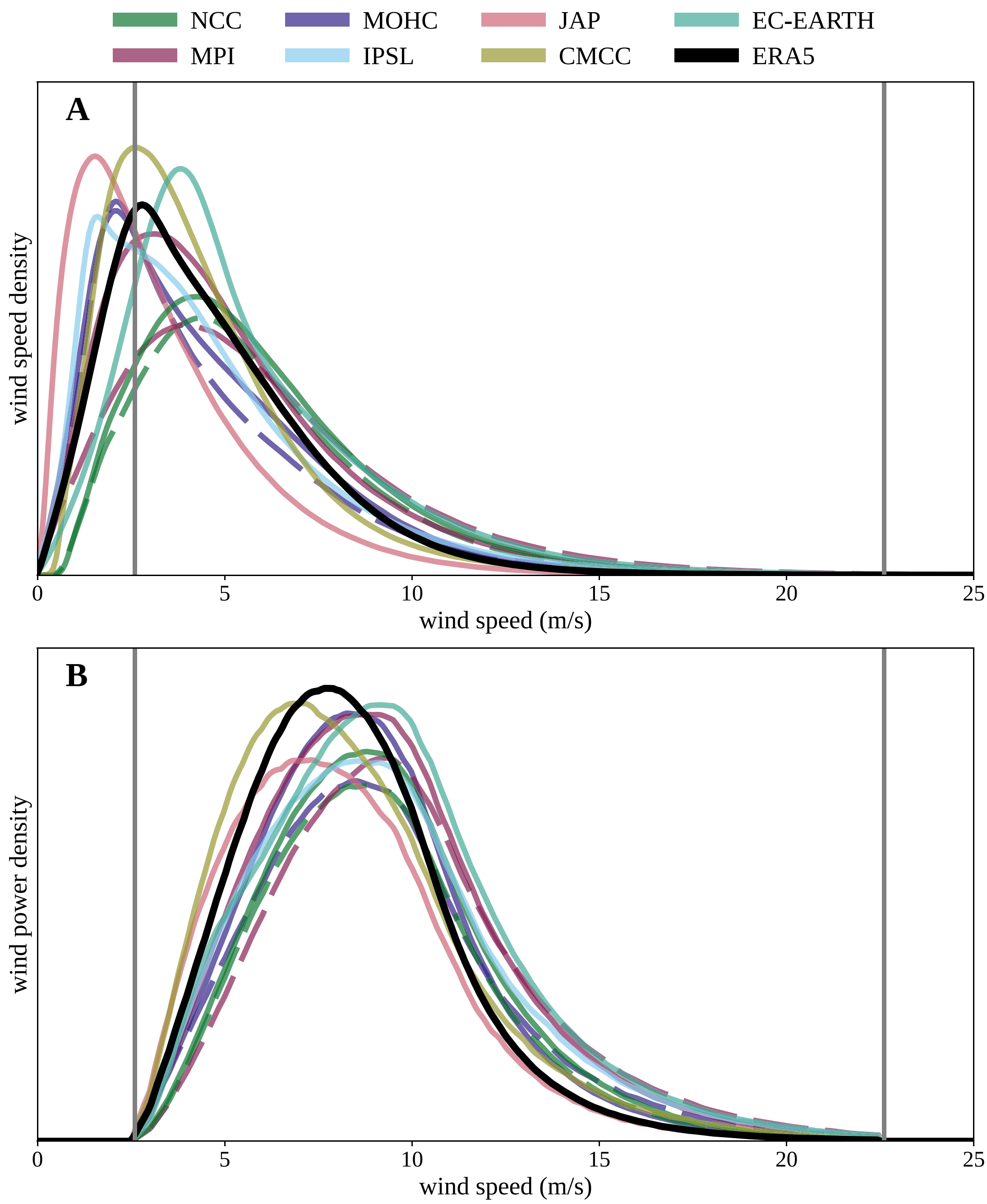

Figure A.1. Extension of figure 3: Kernel density estimations (KDEs) of the wind speeds (A) and the corresponding generated wind power density (B) of all GCM datasets.

A.3. Extended wind power analysis

A.3.1. Robustness to turbine types

To assess the robustness of our wind power analysis, we extend it to different wind turbine types listed in table A.5. The cumulative wind power output for these turbine models is shown in figure A.2.

Table A.5. Characteristics of various turbines organized by subfigure label (first column); including the turbine type (second column), where the last component of the name specifies the rated power in MW, the hub height (third column), the cut-in wind speed w_i (fourth column), and the cut-off wind speed w_o (fifth column). The first turbine (A) corresponds to the one used in the main text.

Subfigure	Turbine Type	Hub Height (m)	w_i (m s^{-1})	w_o (m s^{-1})
A	`Enercon E70-2.00`	85	2.1	25.1
B	`Vestas V126-3.45`	126	2.6	22.6
C	`Vestas V164-9.50`	14	3.1	24.6

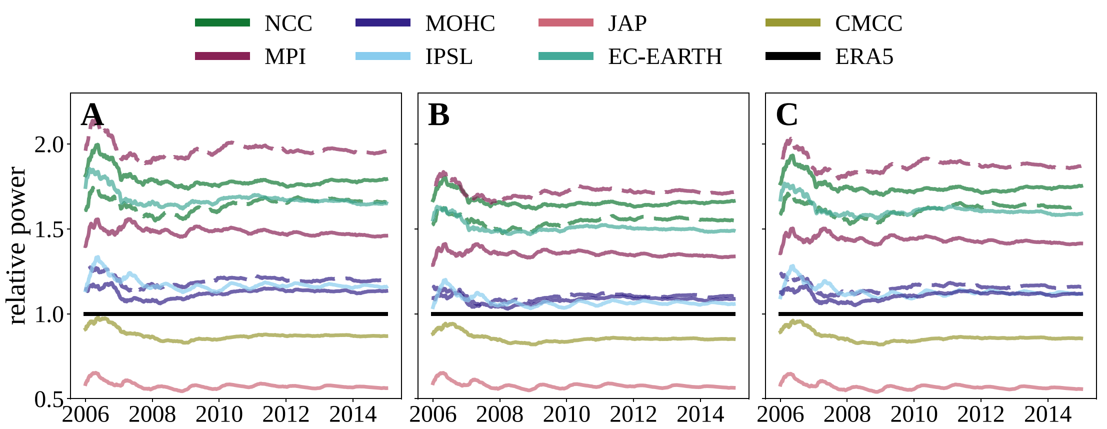

Figure A.2. Extension of figure 6: cumulative wind power of CMIP6 datasets relative to ERA5 for different turbine types given in table A.5.

A.3.2. Analysis of power curve extremes

This section examines the occurrence of wind speeds below the cut-in and above the cut-off thresholds, as these directly affect wind power generation.

A.3.2.1. Logit-transformed extremes

In the context of wind power generation, the cut-in and cut-off wind speeds are the relevant extremes, as they define the thresholds for power generation. Therefore, we also analyze these values and their relationship to spatial resolution. Specifically, we focus on the percentage of wind speeds below cut-in and above the cut-off thresholds, respectively. Although these wind speeds are not considered extreme from a meteorological perspective, they are critical for wind power assessment, as they result in zero power generation.

Given the bounded nature of our dependent variable, directly regressing the proportion of extremes onto the number of data points in each dataset violates key assumptions of linear regression. Since the dependent variable is a proportion or percentage, its relationship is not linear, but rather sigmoidal, with diminishing or accelerating effects as it approaches the bounds of 0 and 1.

To resolve this issue, we apply a logit transformation to the dependent variable, i.e. taking the log of the odds ratio using

$$\mathrm{logit}\,(p) = \ln\left(\frac{p}{1-p}\right) \tag{10}$$

which maps p from the interval $(0,1)$ to $(-\infty,\infty)$. This transformation linearizes the relationship between the predictor and the predictand, allowing for a statistically valid regression analysis.

A.3.2.2. Logit-transformed linear regression results

Figures A.3 and A.4 show the linear regression between the log odds of zero power generation and spatial resolution. Although the figures reveal significant disparities in the dependent variable across models, no systematic trend is found in the linear regression analysis. The regression for three different turbine types each are not statistically significant, see tables A.6 and A.7.

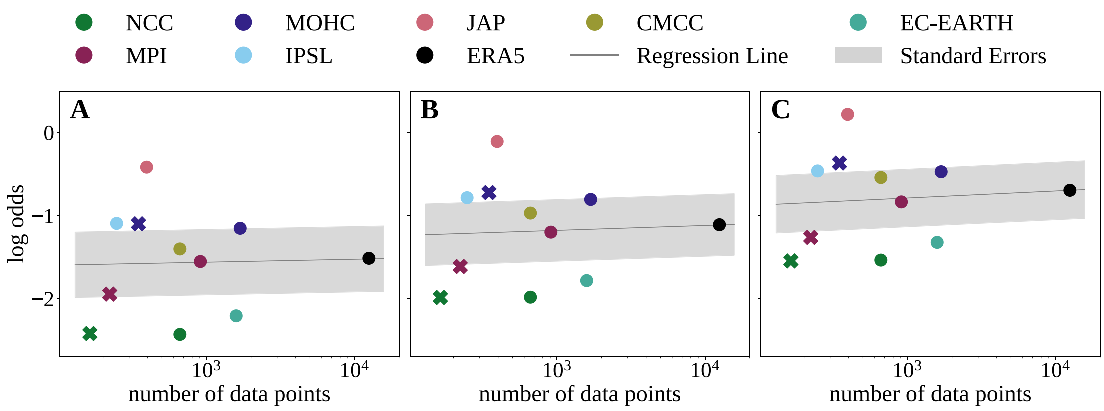

Figure A.3. The log odds of zero power values due to wind speed values below the cut-in wind speed (w_i) are plotted against the spatial resolution. Each dot represents a climate model, labeled in the legend. Results for different wind turbines are displayed in separate subplots. Details of turbine types and their respective cut-in wind speed values are provided in table A.5. The linear-log regression lines are shown in dark grey, with the standard deviation represented as the light grey area; none of the regressions is statistically significant (see table A.6).

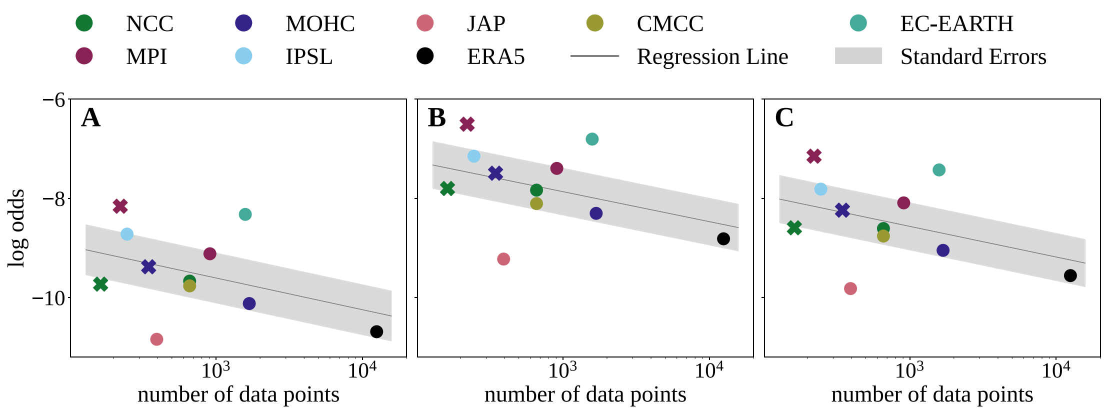

Figure A.4. The log-odds of zero power output due to wind speeds above the cut-off wind speed (w_o) are plotted against the spatial resolution. Each dot represents a climate model, labeled in the legend. Results for different wind turbines are displayed in separate subplots. Details of turbine types and their respective cut-off wind speed values are provided in table A.5. The linear-log regression lines are shown in dark grey, with the standard deviation represented as the light grey area; none of the regressions is statistically significant (see table A.7).

Table A.6. Regression details for the log odds of zero power values due to wind speed values below the cut-in in figure A.3 organized by subfigure label (first column); including the same regression parameters as in table A.4.

Subfigure	Intercept α	Slope β	Std. Dev.	R^2	p-value
A	−1.667	0.036	0.394	0.090	0.9301
B	−1.355	0.059	0.371	0.282	0.8769
C	−1.042	0.085	0.346	0.660	0.8123

Table A.7. Regression details for the log odds of zero power values due to wind speed values above the cut-off in figure A.4 organized by subfigure label (first column); including the same regression parameters as in table A.4.

Subfigure	Intercept α	Slope β	Std. Dev.	R^2	p-value
A	−7.684	−0.640	0.503	15.220	0.2356
B	−6.050	−0.604	0.470	15.512	0.2307
C	−6.709	−0.618	0.475	15.809	0.2259

ORCID iDs

Sofia Morelli https://orcid.org/0009-0006-4850-1455
Nina Effenberger https://orcid.org/0000-0002-0713-1164
Luca Schmidt https://orcid.org/0009-0000-9090-2005
Nicole Ludwig https://orcid.org/0000-0003-3230-8918

References

Arjovsky M, Chintala S and Bottou L 2017 Wasserstein generative adversarial networks *Int. Conf. on Machine Learning* (PMLR) pp 214–23

Barthelmie R J, Shepherd T J, Aird J A and Pryor S C 2020 Power and wind shear implications of large wind turbine scenarios in the us central plains *Energies* **13** 4269

Beniston M *et al* 2007 Future extreme events in European climate: an exploration of regional climate model projections *Clim. Change* **81** 71–95

Bentsen M *et al* 2019 NCC NorESM2-MM model output prepared for CMIP6 CMIP historical (available at: https://doi.org/10.22033/ESGF/CMIP6.8040)

Boucher O *et al* 2018 IPSL IPSL-CM6A-LR model output prepared for CMIP6 CMIP historical (available at: https://doi.org/10.22033/ESGF/CMIP6.5195)

Copernicus Climate Change Service 2019 CORDEX regional climate model data on single levels (available at: https://cds.climate.copernicus.eu/cdsapp#!/dataset/projections-cmip5-r1i1p1) (Accessed 4 September 2024)

EC-Earth 2019 EC-Earth-Consortium EC-Earth3 model output prepared for CMIP6 CMIP historical (available at: https://doi.org/10.22033/ESGF/CMIP6.4700)

Effenberger N and Ludwig N 2022 A collection and categorization of open-source wind and wind power datasets *Wind Energy* **25** 1659–83

Effenberger N, Ludwig N and White R H 2023 Mind the (spectral) gap: how the temporal resolution of wind data affects multi-decadal wind power forecasts *Environ. Res. Lett.* **19** 014015

Endres M D and Schindelin J E 2003 A new metric for probability distributions *IEEE Trans. Inf. Theory* **49** 1858–60

Eyring V, Bony S, Meehl G A, Senior C A, Stevens B, Stouffer R J and Taylor K E 2016 Overview of the Coupled Model Intercomparison Project Phase 6 (CMIP6) experimental design and organization *Geosci. Model Dev.* **9** 1937–58

François B, Vrac M, Cannon A J, Robin Y and Allard D 2020 Multivariate bias corrections of climate simulations: which benefits for which losses? *Earth Syst. Dyn.* **11** 537–62

Giorgetta M *et al* 2012 CMIP5 simulations of the max planck institute for meteorology (MPI-M) based on the MPI-ESM-LR model: the historical experiment, served by ESGF (available at: https://doi.org/10.1594/WDCC/CMIP5.MXELhi)

Giorgi F and Gutowski W J 2015 Regional dynamical downscaling and the CORDEX initiative *Ann. Rev. Environ. Resources* **40** 467–90

Gualtieri G 2021 Reliability of era5 reanalysis data for wind resource assessment: a comparison against tall towers *Energies* **14** 4169

Haas S *et al* 2024 wind-python/windpowerlib: update release (available at: https://doi.org/10.5281/zenodo.10685057)

Hahmann A N *et al* 2020 The making of the new European wind atlas–part 1: model sensitivity *Geosci. Model Dev.* **13** 5053–78

Hersbach H *et al* 2020 The ERA5 global reanalysis *Q. J. R. Meteorol. Soc.* **146** 1999–2049

IEA Internationl energy agency (available at: www.iea.org/energy-system/renewables/wind#) (Accessed 13 August 2024)

Isphording R N, Alexander L V, Bador M, Green D, Evans J P and Wales S 2024 A standardized benchmarking framework to assess downscaled precipitation simulations *J. Clim.* **37** 1089–110

Jungclaus J *et al* 2019 MPI-M MPI-ESM1.2-HR model output prepared for CMIP6 CMIP historical (available at: https://doi.org/10.22033/ESGF/CMIP6.6594)

Kaspar F *et al* 2020 Regional atmospheric reanalysis activities at Deutscher Wetterdienst: review of evaluation results and application examples with a focus on renewable energy *Adv. Sci. Res.* **17** 115–28

Klaver R, Haarsma R, Vidale P L and Hazeleger W 2020 Effective resolution in high resolution global atmospheric models for climate studies *Atmos. Sci. Lett.* **21** e952

Ko O, Vo A, Ah F and Ow I 2022 Projected changes in wind energy potential using CORDEX ensemble simulation over West Africa *Meteorol. Atmos. Phys.* **134** 48

Lovato T and Peano D 2020 CMCC CMCC-CM2-SR5 model output prepared for CMIP6 CMIP historical (available at: https://doi.org/10.22033/ESGF/CMIP6.3825)

Lucas-Picher P *et al* 2021 Convection-permitting modeling with regional climate models: latest developments and next steps *Wiley Interdiscip. Rev.- Clim. Change* **12** e731

MacLeod D, Torralba V, Davis M and Doblas-Reyes F 2018 Transforming climate model output to forecasts of wind power production: how much resolution is enough? *Meteorol. Appl.* **25** 1–10

Maraun D 2016 Bias correcting climate change simulations-a critical review *Curr. Clim. Change Rep.* **2** 211–20

Miao H, Haiming X, Huang G and Yang K 2023 Evaluation and future projections of wind energy resources over the Northern Hemisphere in CMIP5 and CMIP6 models *Renew. Energy* **211** 809–21

Moemken J, Reyers M, Buldmann B and Pinto J G 2016 Decadal predictability of regional scale wind speed and wind energy potentials over Central Europe *Tellus A* **68** 29199

Molina M O, António Martins Careto J ao, Gutiérrez C, Sánchez E and Soares P M M 2022 The added value of high-resolution EURO-CORDEX simulations to describe daily wind speed over Europe *Int. J. Climatol.* **43** 1062–78

Molina M O, Gutiérrez C and Sánchez E 2021 Comparison of ERA5 surface wind speed climatologies over Europe with observations from the HadISD dataset *Int. J. Climatol.* **41** 4864–78

Montgomery D C, Peck E A and Geoffrey Vining G 2021 *Introduction to Linear Regression Analysis* (Wiley)

Ndiaye A, Saley Moussa M, Dione C, Sawadogo W, Bliefernicht J, Dungall L and Kunstmann H 2022 Projected changes in solar PV and wind energy potential over West Africa: an analysis of CORDEX-CORE simulations *Energies* **15** 9602

Olauson J 2018 ERA5: The new champion of wind power modelling? *Renew. Energy* **126** 322–31

Outten S and Sobolowski S 2021 Extreme wind projections over Europe from the euro-cordex regional climate models *Weather Clim. Extremes* **33** 100363

Peterson E W and Hennessey J P 1978 On the use of power laws for estimates of wind power potential *J. Appl. Meteorol. Climatol.* **17** 390–4

Pryor S C, Barthelmie R J, Bukovsky M S, Ruby Leung L and Sakaguchi K 2020 Climate change impacts on wind power generation *Nat. Rev. Earth Environ.* **1** 627–43

Pryor S C, Coburn J J, Barthelmie R J and Shepherd T J 2023 Projecting future energy production from operating wind farms in North America. Part I: dynamical downscaling *J. Appl. Meteorol. Climatol.* **62** 63–80

Pryor S C, Nikulin G and Jones C 2012 Influence of spatial resolution on regional climate model derived wind climates *J. Geophys. Res.: Atmos.* **117** 22

Ramon J, Lledó L, Torralba V, Soret A and Doblas-Reyes F J 2019 What global reanalysis best represents near-surface winds? *Q. J. R. Meteorol. Soc.* **145** 3236–51

Randall D A *et al* 2007 Climate models and their evaluation *Climate Change 2007: The Physical Science Basis. Contribution of Working Group I to the Fourth Assessment Report of the IPCC (FAR)* (Cambridge University Press) pp 589–662

Ridley J, Menary M, Kuhlbrodt T, Andrews M and Andrews T 2019a MOHC HadGEM3-GC31-MM model output prepared for CMIP6 CMIP historical (available at: https://doi.org/10.22033/ESGF/CMIP6.6112)

Ridley J, Menary M, Kuhlbrodt T, Andrews M and Andrews T 2019b MOHC HadGEM3-GC31-LL model output prepared for CMIP6 CMIP historical (available at: https://doi.org/10.22033/ESGF/CMIP6.6109)

Rummukainen M 2016 Added value in regional climate modeling *Wiley Interdiscip. Rev.- Clim. Change* **7** 145–59

Schmidt L and Ludwig N 2024 Wind power assessment based on super-resolution and downscaling–a comparison of deep learning methods (arXiv:2407.08259)

Schulzweida U 2023 CDO user guide (available at: https://doi.org/10.5281/zenodo.10020800)

Scott D W 2010 Scott's rule *Wiley Interdiscip. Rev.- Comput. Stat.* **2** 497–502

Seland Øyvind *et al* 2019 NCC NorESM2-LM model output prepared for CMIP6 CMIP historical (available at: https://doi.org/10.22033/ESGF/CMIP6.8036/)

Shu Z R and Jesson M 2021 Estimation of Weibull parameters for wind energy analysis across the UK *J. Renew. Sustain. Energy* **13** 1

Staffell I and Pfenninger S 2016 Using bias-corrected reanalysis to simulate current and future wind power output *Energy* **114** 1224–39

Tatebe H and Watanabe M 2018 MIROC MIROC6 model output prepared for CMIP6 CMIP historical (available at: https://doi.org/10.22033/ESGF/CMIP6.5603)

Taylor K E, Stouffer R J and Meehl G A 2012 An overview of CMIP5 and the experiment design *Bull. Am. Meteorol. Soc.* **93** 485–98

Vautard R *et al* 2021 Evaluation of the large EURO-CORDEX regional climate model ensemble *J. Geophys. Res.: Atmos.* **126** e2019JD032344

Wieners K-H *et al* MPI-M MPI-ESM1.2-LR model output prepared for CMIP6 CMIP historical (available at: https://doi.org/10.22033/ESGF/CMIP6.6595)

Wohland J, Omrani N-E, Witthaut D and Keenlyside N S 2019 Inconsistent wind speed trends in current twentieth century reanalyses *J. Geophys. Res. Atmos.* **124** 1931–40

Yu B, Zhang X, Li G and Yu. W 2022 Interhemispheric asymmetry of climate change projections of boreal winter surface winds in canesm5 large ensemble simulations *Clim. Change* **170** 23

Zhang Z and Wang K 2024 Quantify uncertainty in historical simulation and future projection of surface wind speed over global land and ocean *Environ. Res. Lett.* **19** 054029